3.1.9.2 Pilot-point Calibration Approach. An alternative inverse modeling approach, namely the pilot-point approach, was also implemented to calibrate the two-dimensional flow model using the same June 2004 head data. Figure 3-14 shows the distribution of the pilot points. The overall strategy of selecting the pilot points is to distribute the pilot points uniformly first and then refine the distribution in areas with a large head gradient. We also refine the distribution of pilot points near facilities such as INTEC, TAN, and RWMC, where observation wells are highly concentrated. A total of 265 pilot points is distributed within the domain. PEST estimates the K values at these pilot points and then interpolates the estimated K values to each active grid cell within the domain.

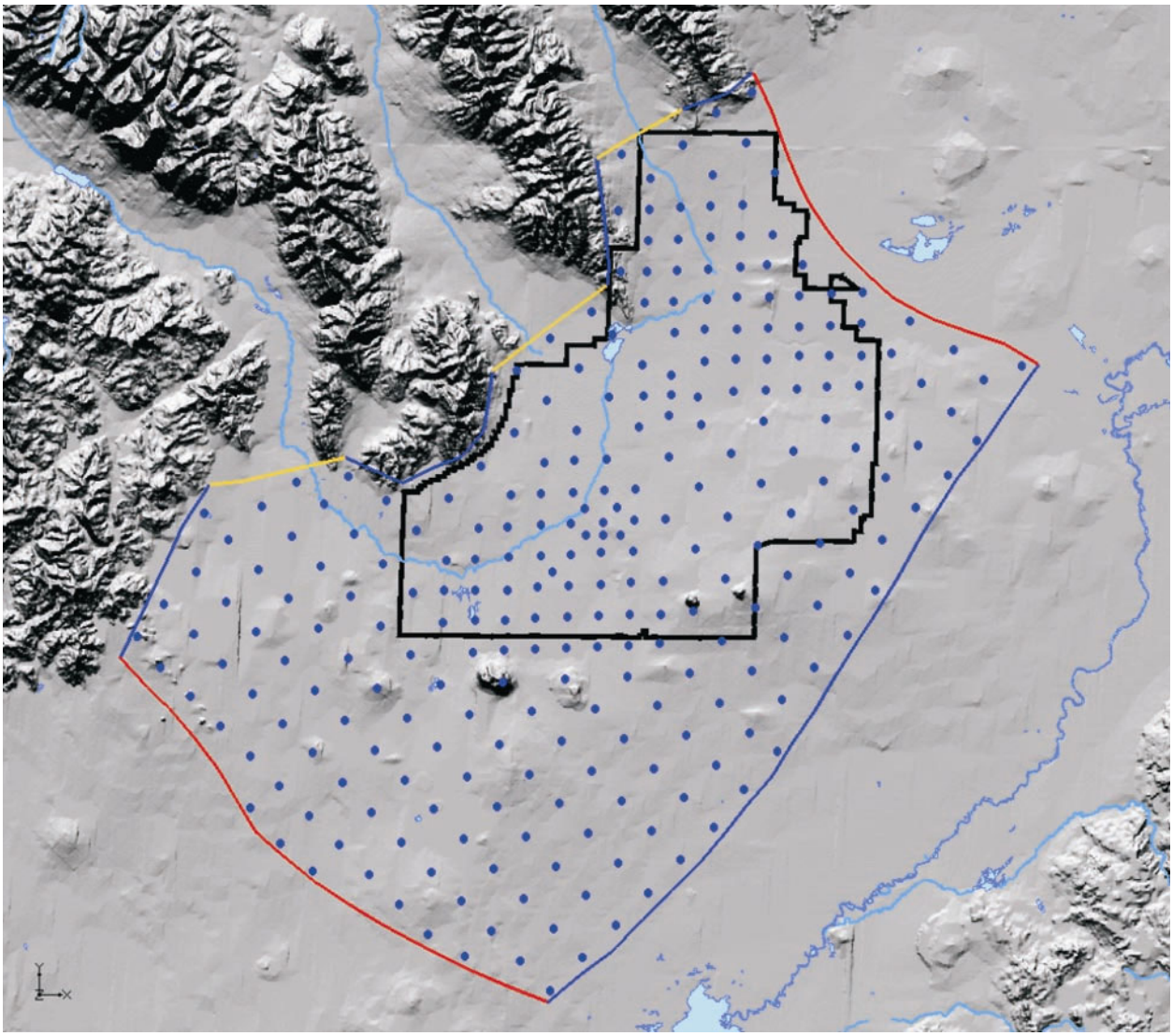

Figure 3-14. Distribution of pilot points.

Like the zonation approach, we have implemented the pilot-point method to both thick and thin aquifer scenarios. Initially, we planned to use the pumping test data shown in Figure 2-13 as a subset of pilot points with fixed K values in our two-dimensional flow model. However, we quickly realized that all of those pumping test were performed through limited intervals of wells and did not necessarily represent the averaged K values across the entire aquifer thickness. Furthermore, most tests are just single-well tests and have a limited influence area. Therefore, these test data also have a scale discrepancy

with the model grid size. For these reasons, we decided not to directly use these pumping test data as prior information during the calibration process. Instead, the range of K values inferred from pumping tests was used to set up the upper and lower limits of K value at each pilot point.

We tried to use the pumping test data to infer the variogram of the K field. However, the test data provide a poor estimate of the variogram or correlation structure. We also experienced some numerical instability problems during inversion when an arbitrary variogram was used to krige the K values at pilot points to each grid cell. Therefore, we decided to use a simpler inverse distance method to interpolate K values at pilot points. The nearest five points were selected for interpolation. Such an interpolation scheme yields stable solutions for the thick and thin aquifer scenarios.

Figure 3-15 shows the simulated hydraulic head contour map and residuals at all observation wells for thick and thin aquifer scenarios. Figure 3-16 shows the residuals of observation wells near INTEC and RWMC. As shown in these figures, most observation wells have mismatches less than 2 m (6.5 ft). Only a limited number of wells have mismatches over 2 m (6.5 ft) but still less than 3 m (9.8 ft). Compared with the previous zonation approach, the pilot-point approach not only reproduces the large-scale features of the measured groundwater table but also provides much more satisfactory matches to all measured heads. Figure 3-17 shows the residuals more clearly.

Figure 3-17 shows the residual distributions for the thick and thin aquifer thickness scenarios. Most observation wells have residuals less than 1 m (3.3 ft); only a limited number of wells have residuals greater than 1 m (3.3 ft). The thin aquifer scenario provides slightly better matches (smaller residuals) than the thick aquifer scenario, as manifested by the statistics of residuals shown in this figure.

Figure 3-18 shows the comparison of the estimated hydraulic conductivity maps between two aquifer thickness scenarios. Visual comparison between the two maps reveals some differences in the magnitude of the estimated K values for a number of zones. However, the overall K value distribution patterns are similar for both scenarios. Compared with the zonation approach, the estimated conductivity field using the pilot-point approach looks more realistic and varies more smoothly while still allowing variations at different scales. One interesting point is that the estimated field starts to reflect some known large-scale geological structures.

Figure 3-19 shows the transmissivity fields that result from multiplying the estimated K field by the effective aquifer thickness. Like the zonation approach, the transmissivity fields for both aquifer thickness scenarios look rather similar. This is in agreement with the fact that for a horizontal two-dimensional flow model, the transmissivity field is the primary parameter that determines the head distributions. Although we have used a two-dimensional model with variable aquifer thickness, only transmissivity really matters in terms of affecting simulated head contour maps.

Like the zonation approach, PEST also automatically calculates the confidence bounds of the estimated K value for each pilot point, an indicator of parameter uncertainties. Figure 3-20 shows the estimated K value and corresponding 95% confidence bound of each pilot point for both thick and thin aquifer thickness scenarios. Compared with the zonation approach, the confidence bounds of the estimated K values are much narrower, a strong indicator that the estimated parameter field is well resolved during the inversion process.

In summary, compared with the previous zonation approach, the pilot-point approach is not only able to provide satisfactory matches to all of the measured heads and reproduce large- and local-scale features of the measured groundwater table but is also able to extract more heterogeneity information at various scales using the same amount of measured information. The ability of the model to accurately reproduce both large- and small-scale features of the measured groundwater table is particularly critical to

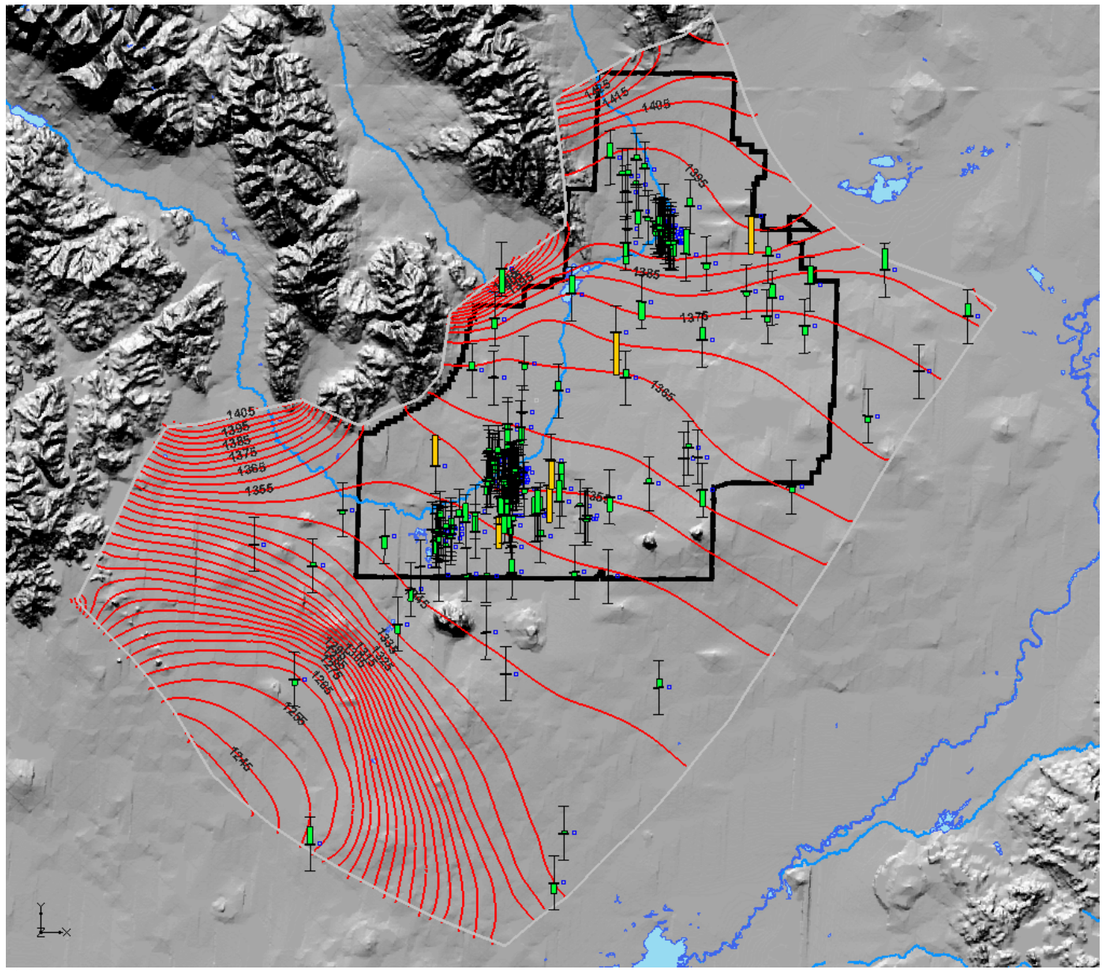

(a)

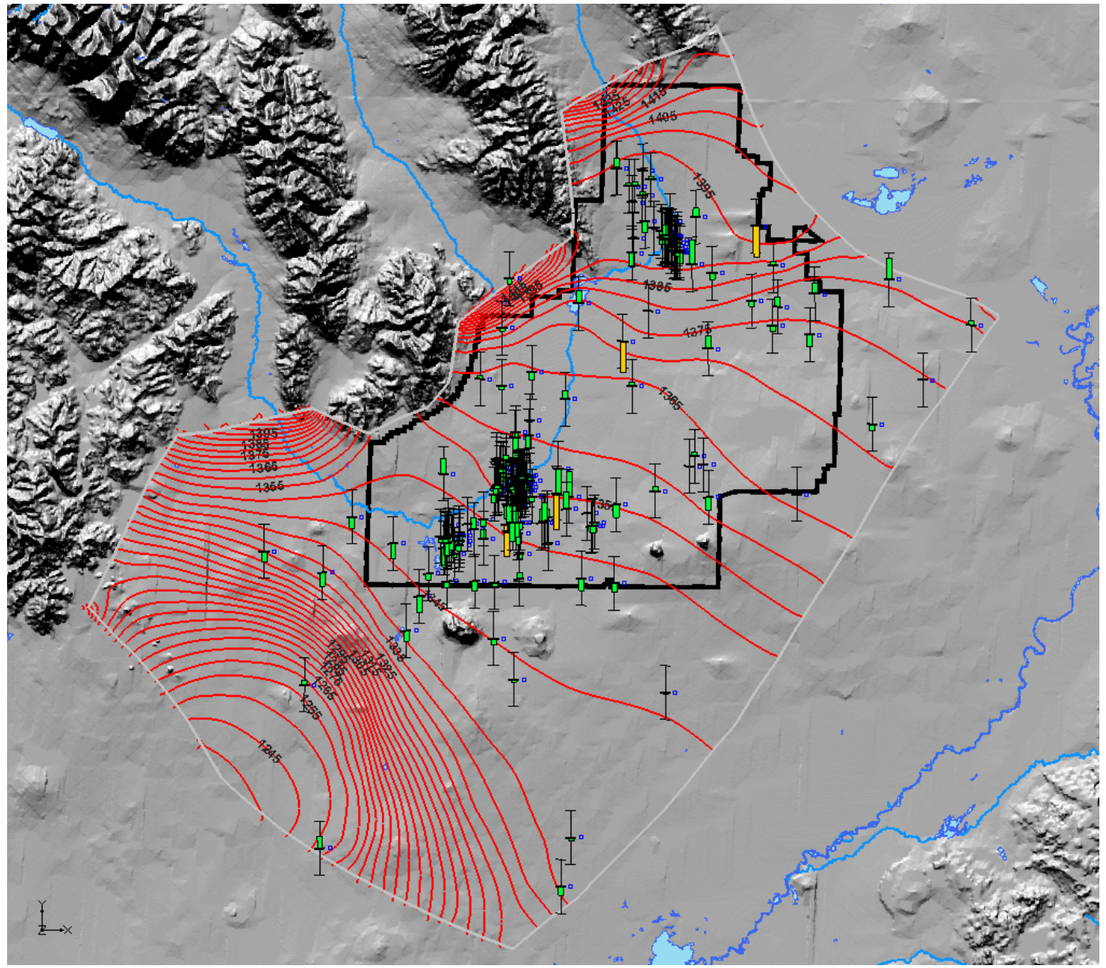

(b)

Figure 3-15. Simulated head contour map and simulation residuals at observation wells for (a) the thick aquifer scenario and (b) the thin aquifer scenario (red is > 3 m, yellow is 2–3 m, and green is < 2 m).

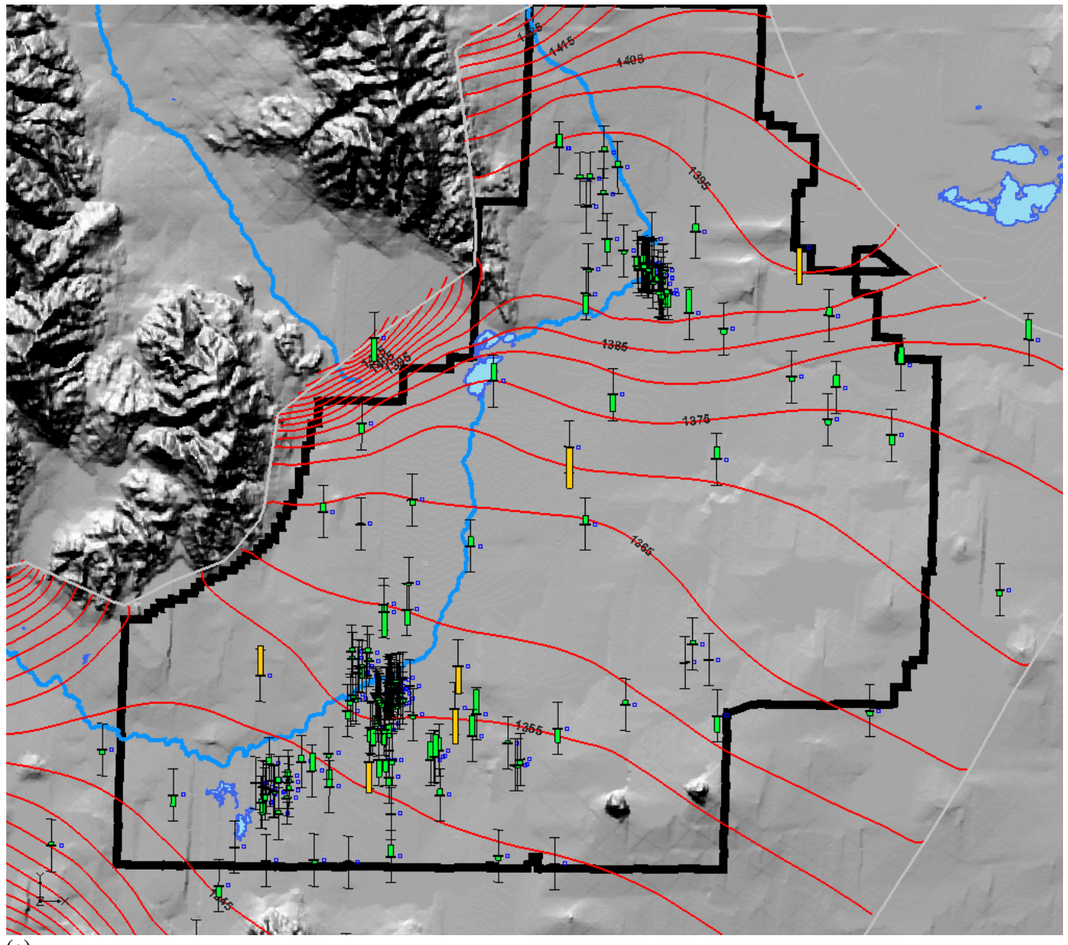

(a)

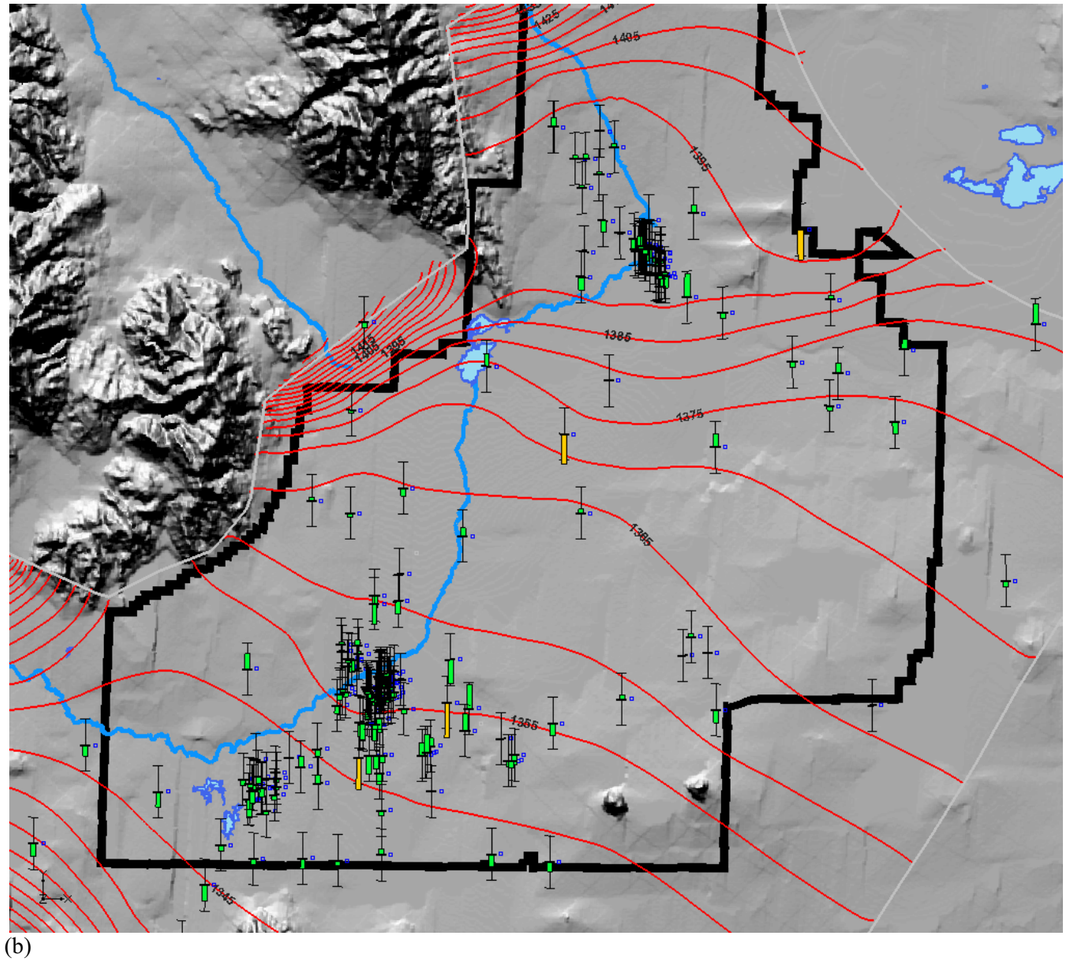

(b)

Figure 3-16. Simulated head contour map and simulation residuals at observation wells inside INL Site for (a) the thick aquifer scenario and (b) the thin aquifer scenario (red is > 3 m, yellow is 2–3 m, and green is < 2 m).

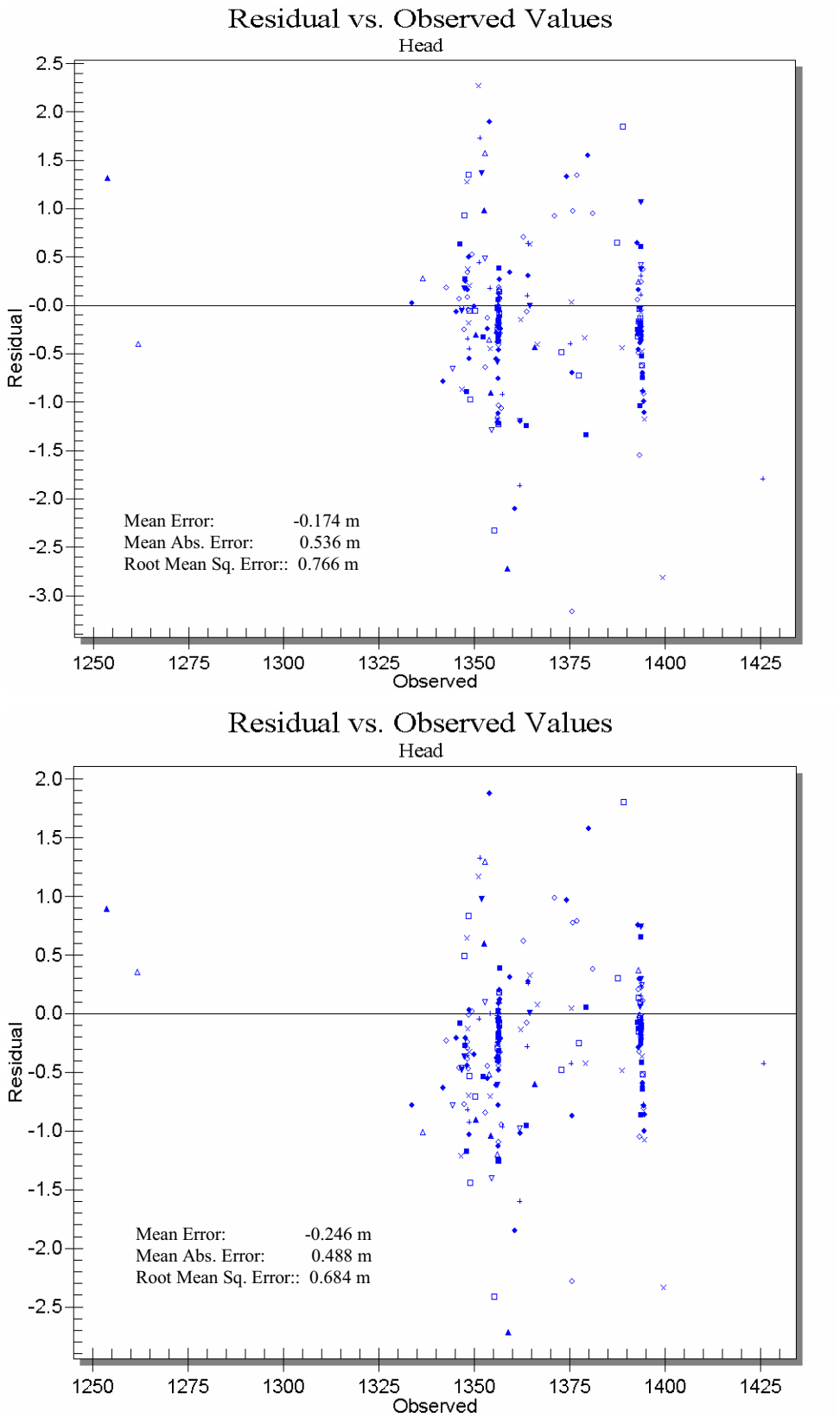

Figure 3-17. Residual versus observed head values for the thick aquifer scenario (top) and the thin aquifer scenario (bottom).

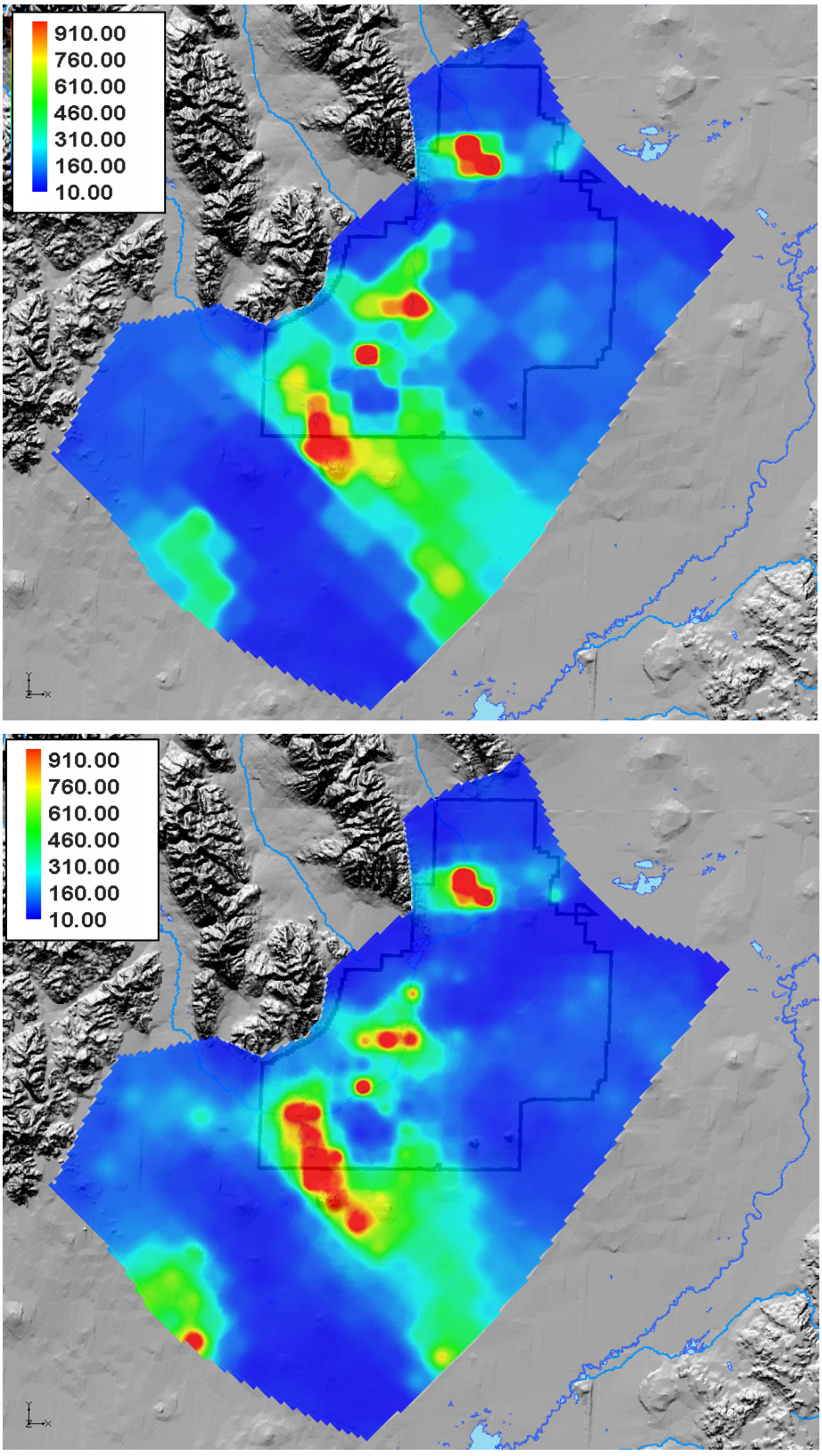

Figure 3-18. The estimated hydraulic conductivity field (in m/d) for the thick scenario (top) and the thin scenario (bottom).

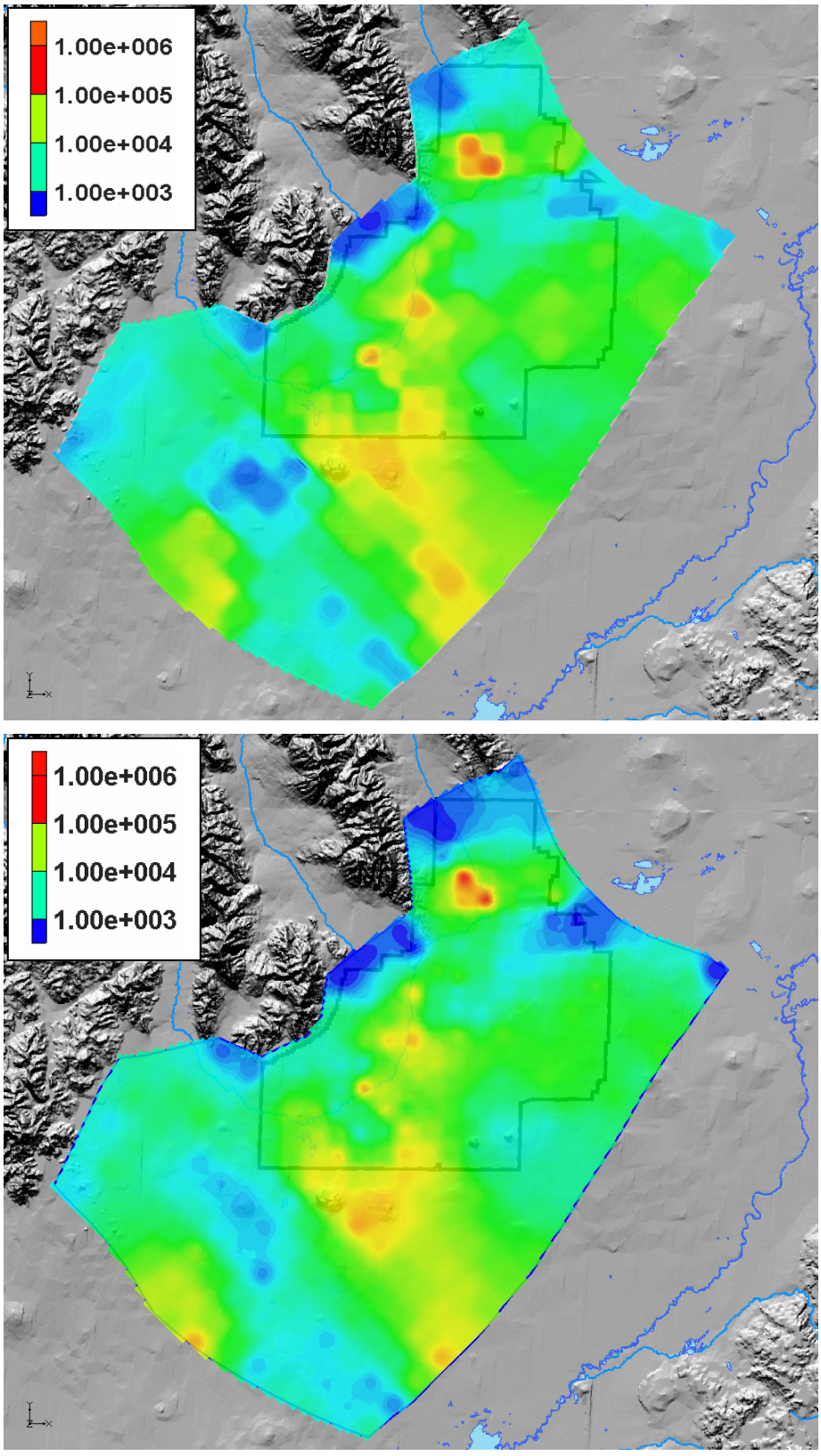

Figure 3-19. The calculated transmissivity field for the thick scenario (top) and the thin scenario (bottom).

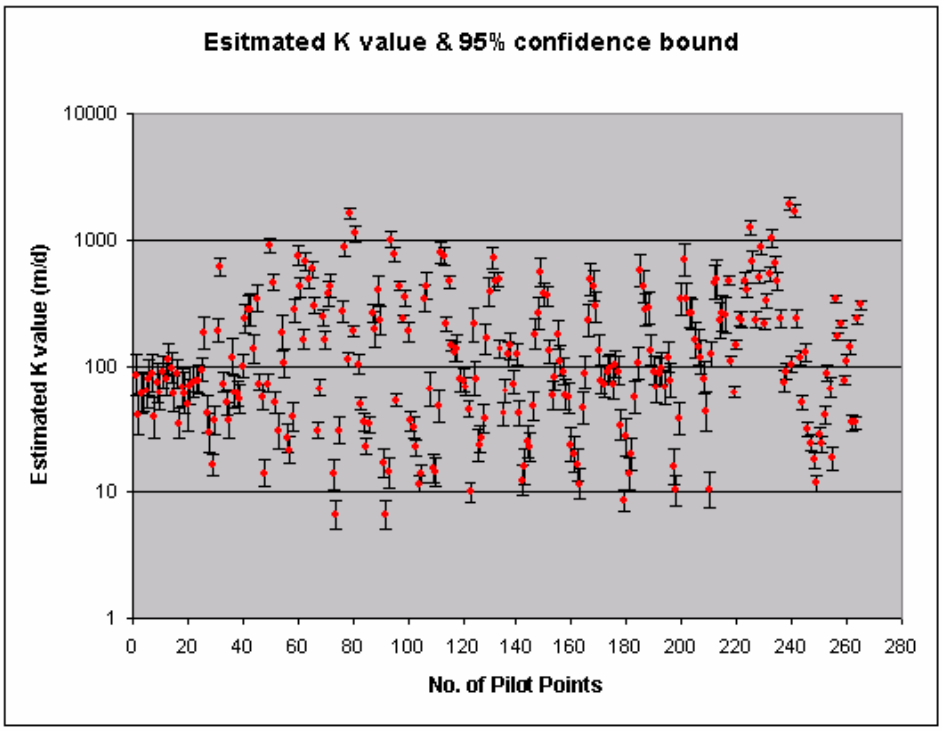

(a)

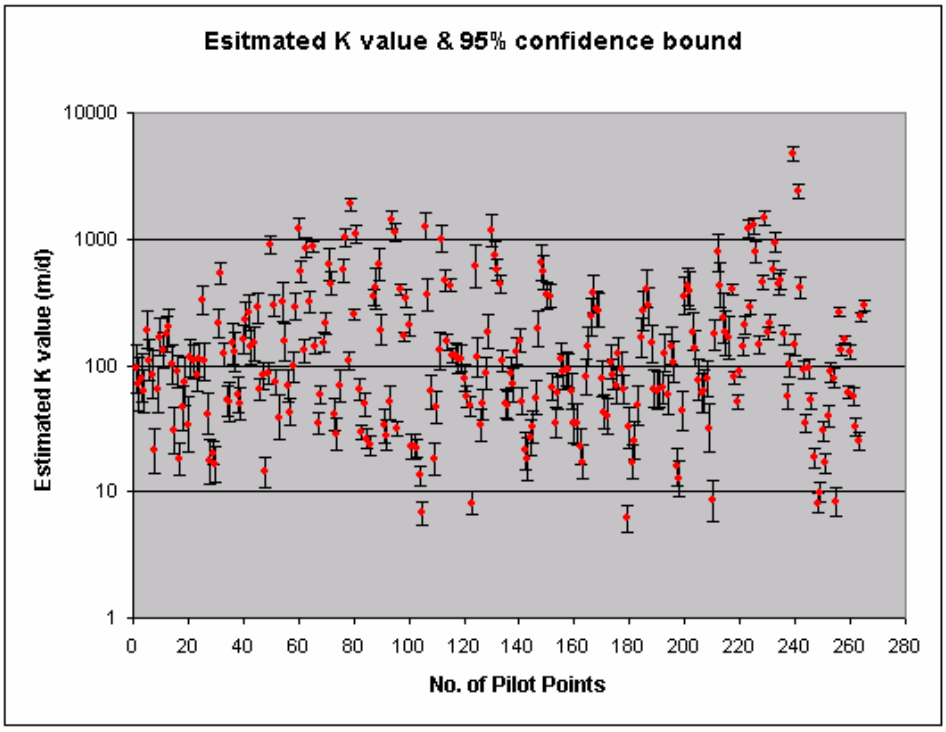

(b)

Figure 3-20. The estimated K values and corresponding 95% confidence bounds of pilot points for (a) the thick aquifer scenario and (b) the thin aquifer scenario.

accurately predict the contaminant migration path inside the INL Site boundaries. In addition, the estimated parameter fields for both aquifer thickness scenarios exhibit low uncertainties, indicating the estimated parameter values are well resolved during the inversion process. All of the results shown previously indicate that the pilot-point approach outperforms the zonation approach.

3.1.9.3 Coupled Zonation/Pilot-point Calibration Approach. The pilot-point approach provides satisfactory results in terms of a better match to the observed heads and more reliable estimates of the parameter field, but this approach is often criticized for not honoring the large-scale geological features. Reliability in this context means the likelihood of being a unique solution. Therefore, we also implemented the coupled zonation/pilot-point approach to calibrate the two-dimensional flow model. In this approach, we still use zones to honor the large-scale geological features and then distribute an independent set of pilot points to each zone to allow sub-zone heterogeneity to be modeled. Ideally, the coupled approach should provide a better result than those for either the zonation approach or pilot-point approach.

A simulation with the coupled zonation/pilot-point approach was carried out in which the geologic subdomains were significantly simplified. The lumping of the subdomains was determined by comparing the June 2004 water table map with the full set of subdomains. Areas where the water table showed no significant response to the subdomain boundaries were found to be hydrogeologically indistinguishable from the surrounding subdomains and were therefore lumped together. Figure 3-21a shows the subdomain map overlain with the interpolated water table contours. One can see that a number of the geologic subdomains are, in effect, invisible to the head contours. Figure 3-21b shows the geologic subdomains lumped into five hydrogeologic complexes. The major geologic features are preserved in the hydrogeologic complexes, such as the Arco Rift, which is contained in the Arco Rift complex that runs completely across the center of the model domain. Each lumped zone contains at least a number of observation wells. In this manner, we honor the geologic constraints on the flow system while numerically capturing the complex hydrogeology. Figure 3-21c shows the individual sets of the pilot points for individual lumped zones. Each zone clearly has its own population and density of pilot points. Interpolation of K values is allowed within each zone but not across zone boundaries. Due to the time limit, we only implemented this approach for the thin aquifer scenario. We expect the thick scenario will yield similar results, as shown previously for the zonation approach and pilot-point approach.

Figure 3-22a shows the simulated hydraulic head contour map and residuals at all observation wells, and Figure 3-22b shows the residuals of observation wells inside the INL Site. As shown in these figures, most observation wells have mismatches of less than 1 m. A few wells have mismatches of about 2 m. Compared with the previous zonation approach and pilot-point approach, the coupled approach seems to provide the best matches to the observed heads, particularly near INTEC.

Figure 3-23 shows the residual distributions. Most observation wells have residuals of less than 1 m (3.3 ft); only a limited number of wells have residuals greater than 1 m (3.3 ft). The statistics of residuals shown in this figure reveal that the coupled approach does provide a slightly better match to the measured heads compared with the pilot-point approach.

Figure 3-24 shows the estimated hydraulic conductivity field generated by the coupled zonation/pilot-point approach. The estimated K field shows overall patterns similar to those shown in the K field estimated by the pilot-point approach. However, a number of discontinuities in the K value exist across the zone boundaries. Sharp changes in the K value across those zone boundaries are clearly shown across the entire domain. Compared with the K field estimated by the pilot-point approach, in which the K value varies smoothly, it is difficult to judge which parameter field is more reliable (or realistic) via visual comparison.

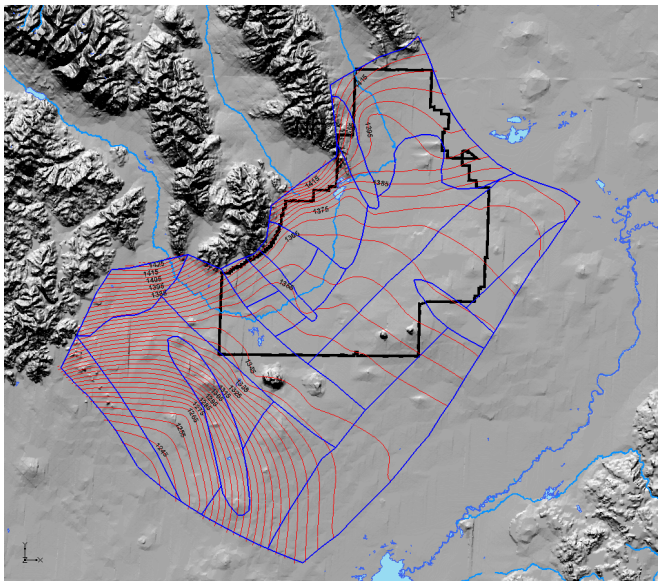

(a)

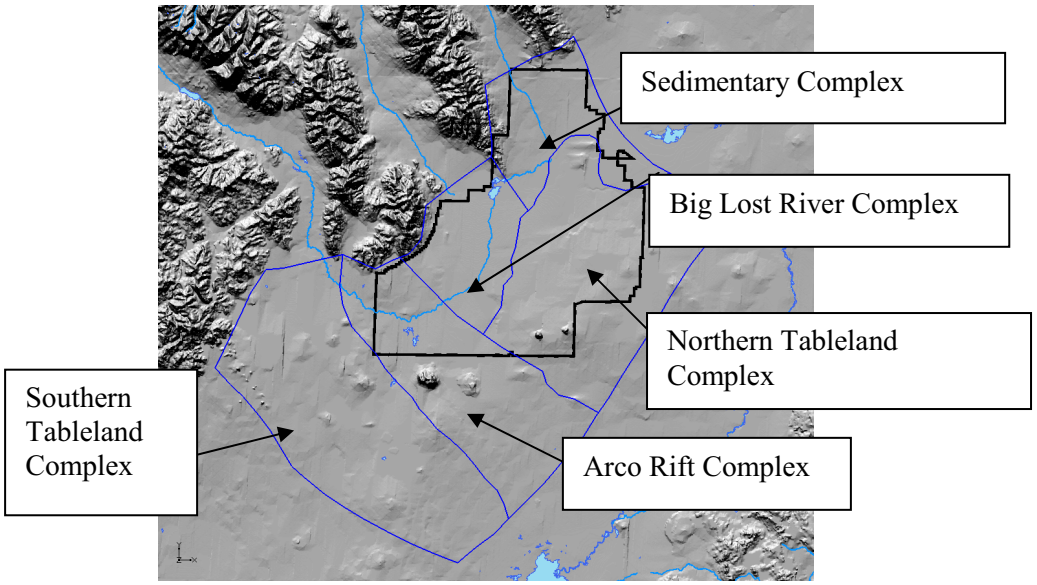

(b)

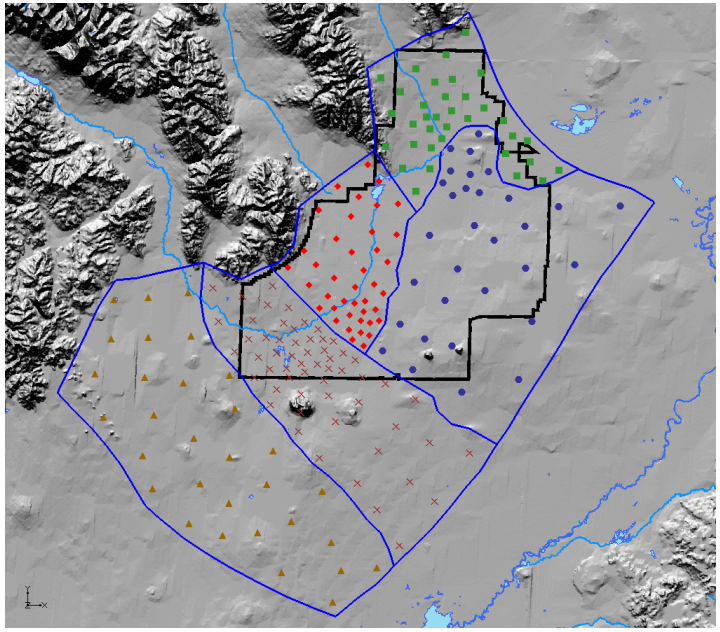

(c)

Figure 3-21. (a) Geologic subdomains overlain with the June 2004 water table (5-m contour interval), (b) the resulting "lumped" subdomains or hydrogeologic complexes, and (c) the pilot-point distributions for individual zones.

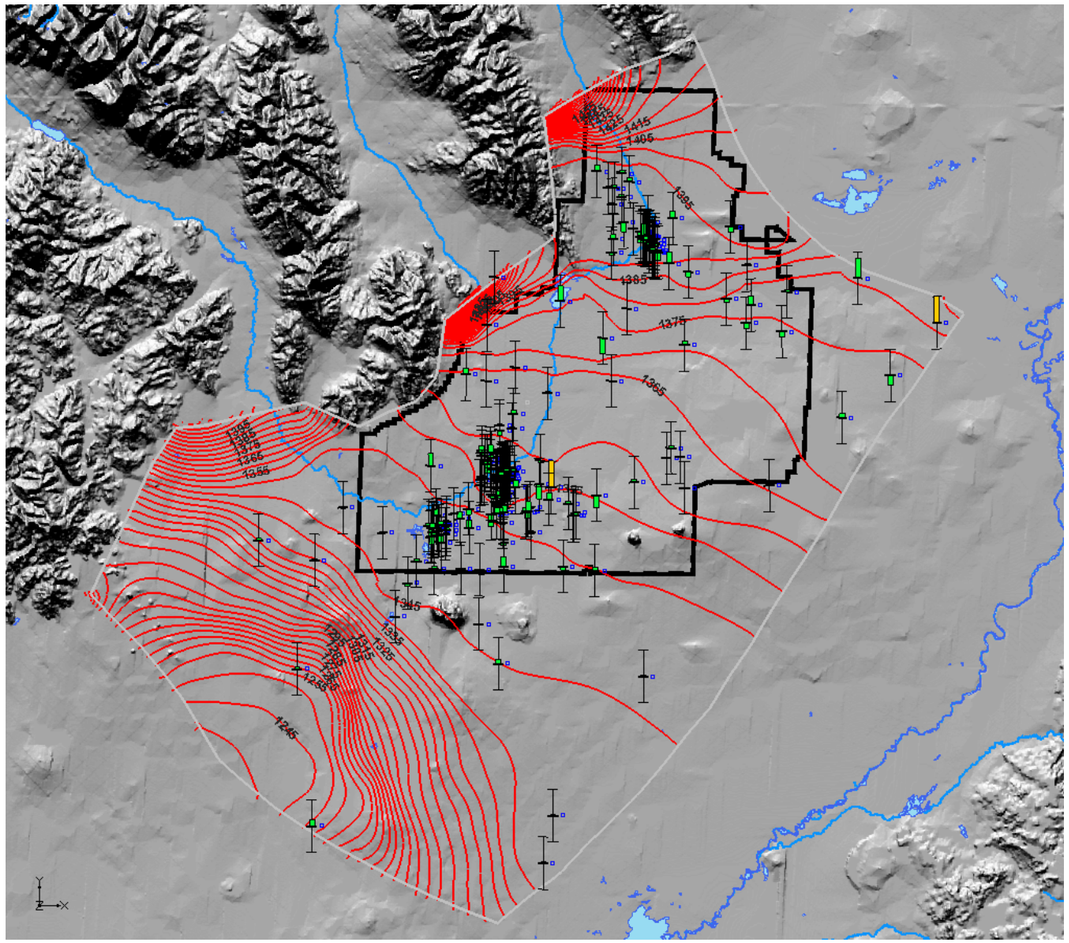

(a)

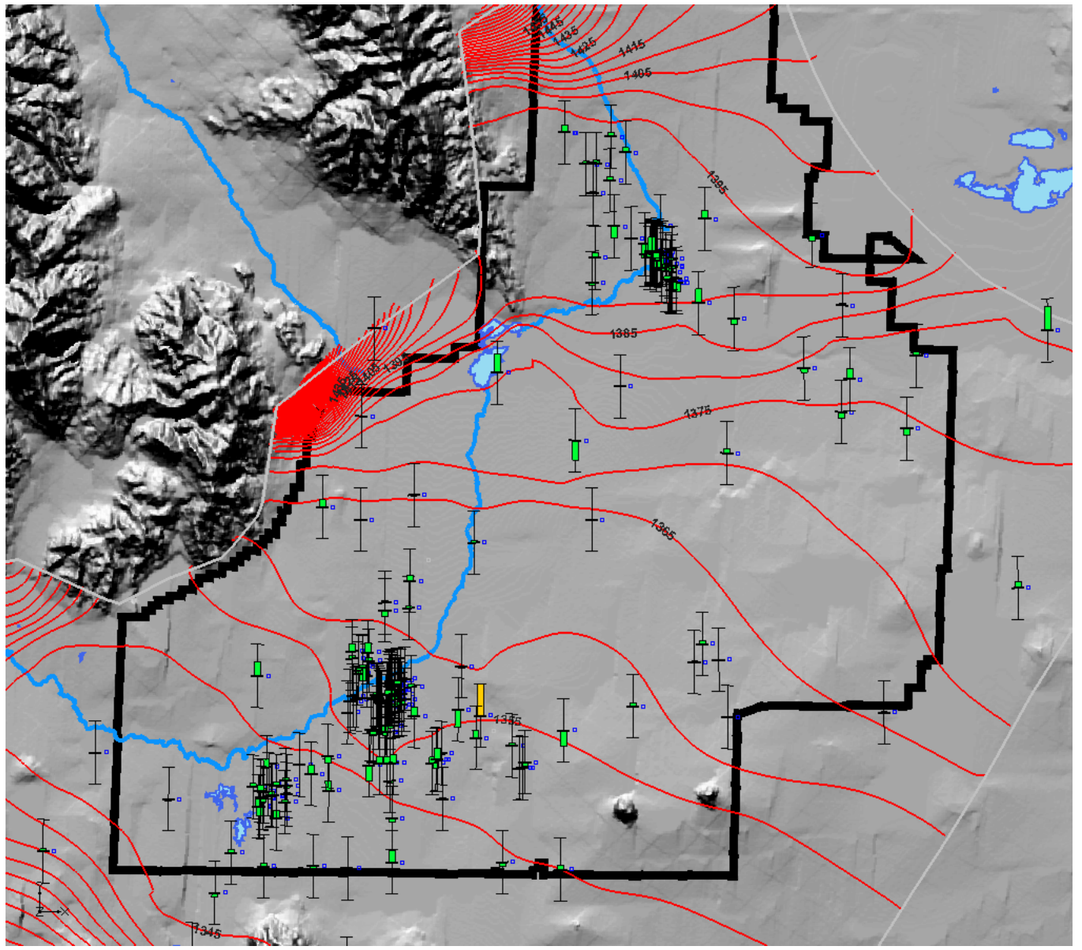

(b)

Figure 3-22. Simulated head contour map and simulation residuals at observation wells for the “thin” aquifer scenario for (a) the whole domain and (b) the central portion of the domain (red is > 3 m, yellow is 2–3 m, and green is < 2 m).

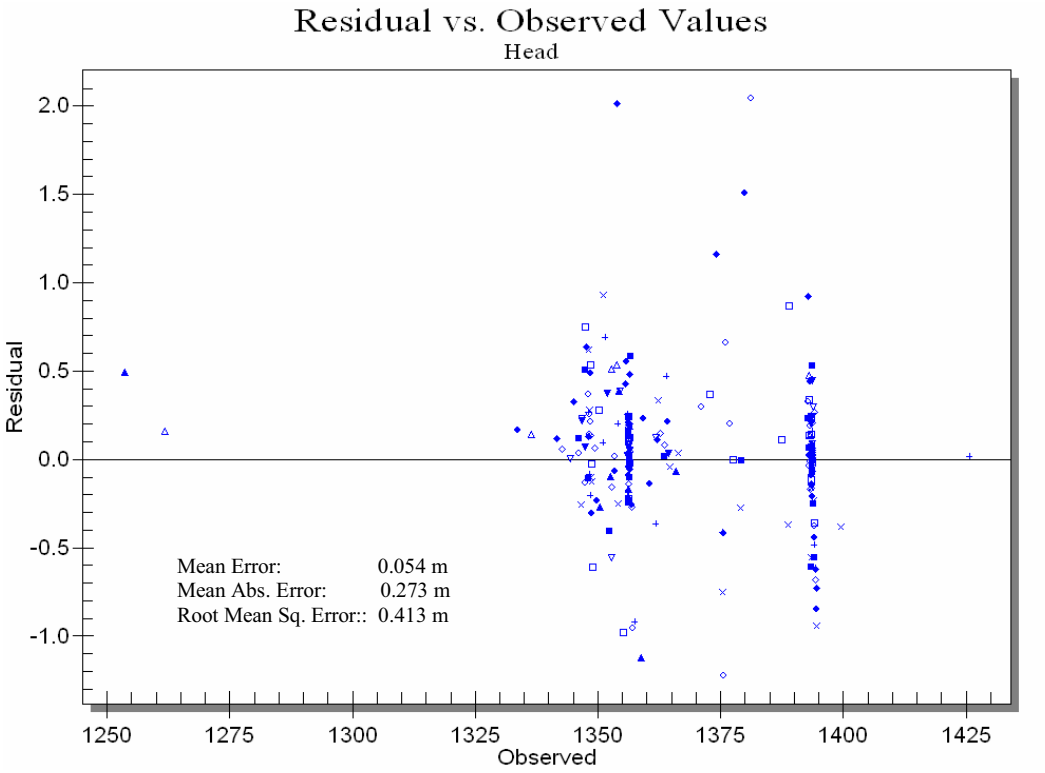

Figure 3-23. Residual versus observed head values.

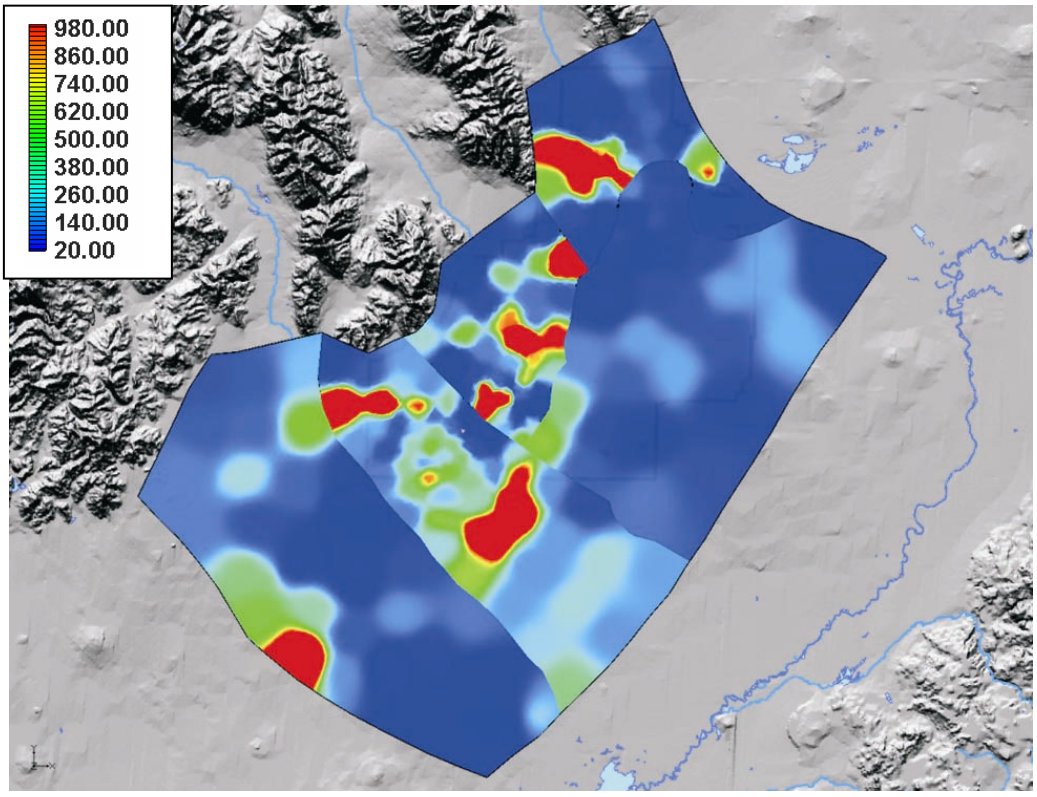

Figure 3-24. The estimated hydraulic conductivity field (m/d).

Like the previous two approaches, we also investigated the reliability of the estimated K field through the parameter confidence bounds (or uncertainty). PEST also automatically calculates the parameter confidence bounds for the coupled zonation/pilot-point approach. Figure 3-25 shows the 95% confidence bounds of the estimated parameter at each pilot point. Many parameters have confidence bounds spanning two to six orders of magnitude. Some parameters have even higher confidence intervals, a strong indicator that the estimated parameter field is much less resolved than that estimated by the pilot-point approach. The large confidence intervals shown in Figure 3-25 also indicate that it is highly likely that the inverse procedure tends to have a non-unique solution. Although the coupled approach provides the best match to the observed heads among all three calibration approaches, the estimated hydraulic conductivity is much less reliable than that obtained by the pilot-point approach.

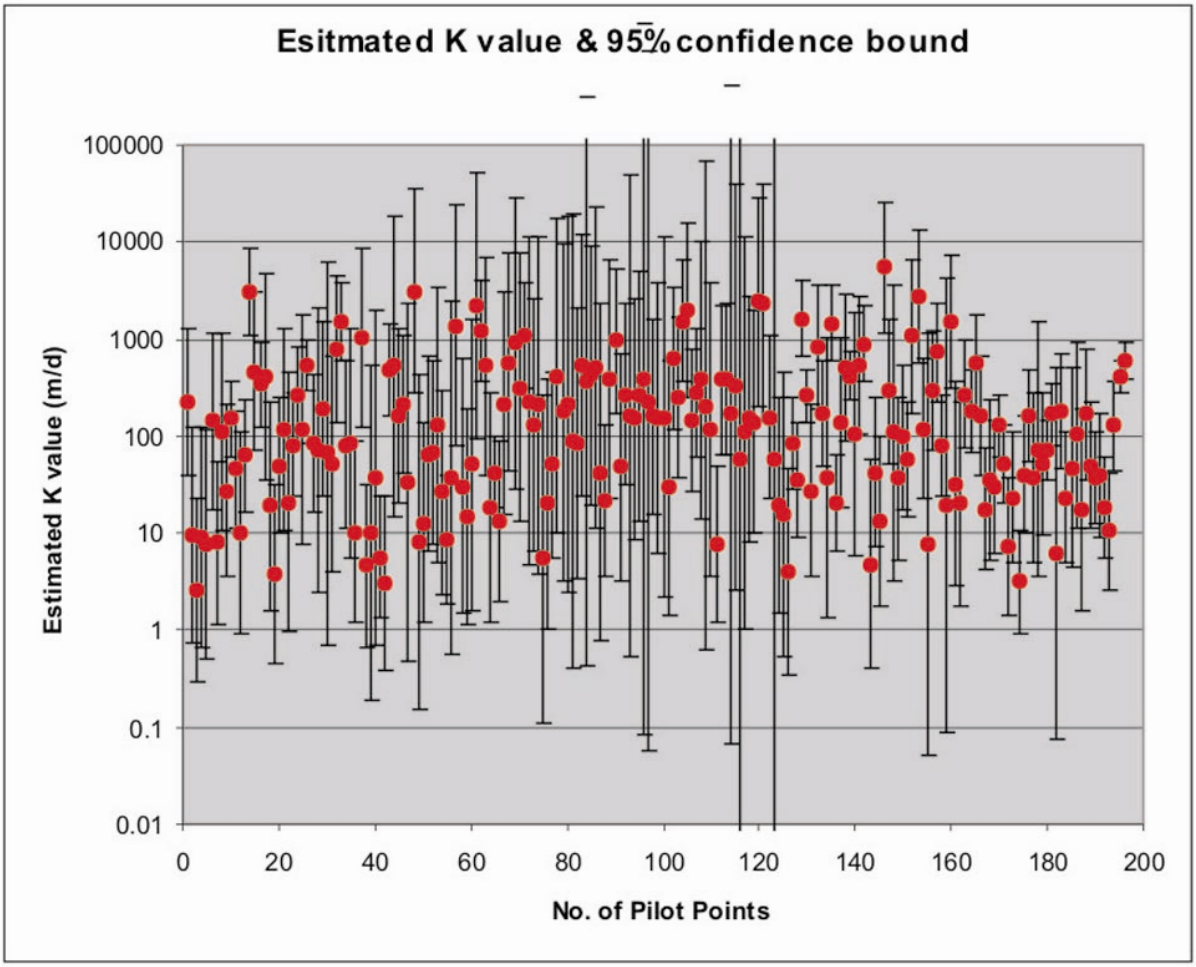

Figure 3-25. The estimated K values and corresponding 95% confidence bounds of pilot.

3.1.10 Sensitivity Analysis

The following subsections summarize the sensitivity studies of the model with respect to hydraulic conductivity values, boundary conditions (tributary underflows), and recharge (including homogeneous and inhomogeneous infiltration of precipitation).

The two-dimensional groundwater flow model is a useful tool for evaluating regional flow in the vicinity of the INL Site, but results inferred from the model must be evaluated with respect to their

sensitivity to various parameters, primarily the hydraulic conductivity, the tributary groundwater underflow rate, and the precipitation recharge rate. Large variations in the hydraulic conductivity field, the underflow rate, and spatial distribution of precipitation recharge rate have been observed or inferred. In the subsections below, we report the sensitivity study of the two-dimensional flow model with respect to the following important model inputs:

- Hydraulic conductivity values
- Estimated underflow rates from the tributary drainage basins
- Homogeneous versus heterogeneous precipitation infiltration.

Because we concluded that the pilot-point approach provides the best results in terms of smallest residuals and most reliable parameters, we used the pilot-point approach for the thin aquifer scenario as our base case for sensitivity studies.

3.1.10.1 Sensitivity Study for the Hydraulic Conductivity. The traditional sensitivity study of the flow model with respect to the hydraulic conductivity is to change the K value by a small amount (i.e., 1%) and then rerun the model and calculate a so-called coefficient of variation by dividing the changes of the simulated heads with the changes of the K value. In our pilot-point approach, however, a total of 265 pilot points were used. Thus, the traditional way to carry out the sensitivity study requires a tremendous amount of effort. We propose an alternative way to carry out the sensitivity study. The composite sensitivity, which basically measures the sensitivity of the objective function (sum of weighted residuals), is calculated with respect to the K value at a particular pilot point. PEST automatically calculates the composite sensitivities during the inversion process.

Figure 3-26 shows the composite sensitivity map of hydraulic conductivity to the objective function. The hydraulic conductivity values in the southern portion of the domain, south of the INL Site boundary, are most sensitive to the simulated heads. One possible reason for the higher composite sensitivity near this area is that this area functions like a gate close to the groundwater exit of the model domain; therefore, small changes in K values in this area will have large impacts on the simulated heads in the central and northern portions of the model domain. Unfortunately, this area only has a few wells to constrain the inversion process. Large uncertainties of K values exist in this area, which eventually will propagate to uncertainties associated with contaminant transport prediction. Inside the INL Site boundaries, the composite sensitivity is fairly uniformly distributed, except for a relatively more sensitive area near the Little Lost River tributary basin.

3.1.10.2 Sensitivity Study for the Underflow Recharge Rate. The two-dimensional flow model includes three underflow recharge boundaries along the west boundary of the model domain. As discussed previously, large uncertainties associated with these estimated fluxes are also expected. We carried out sensitivity studies on these estimated fluxes by changing the estimated flux with a small amount (1%) and calculating the sensitivity coefficients by dividing the corresponding changes of the simulated heads in all grid blocks with the change of the underflow rate. Figures 3-27 through 3-29 are the sensitivity coefficient maps of the simulated heads to the underflow rates from the Big Lost River, Little Lost River, and Birch Creek drainage basins, respectively. All three sensitivity maps are plotted using the same color scale for convenience of comparison.

Visual comparison among these sensitivity maps (using the same color bar scale) immediately reveals that the simulated heads near Birch Creek drainage basin are mostly sensitive to the underflow recharge rate of that basin. In addition, all underflow rates are relatively more sensitive to the heads near drainage basins, but the sensitivity quickly fades away inside the domain. The underflow rate of the Little Lost River drainage basin has slightly higher sensitivity inside the INL Site boundaries than those

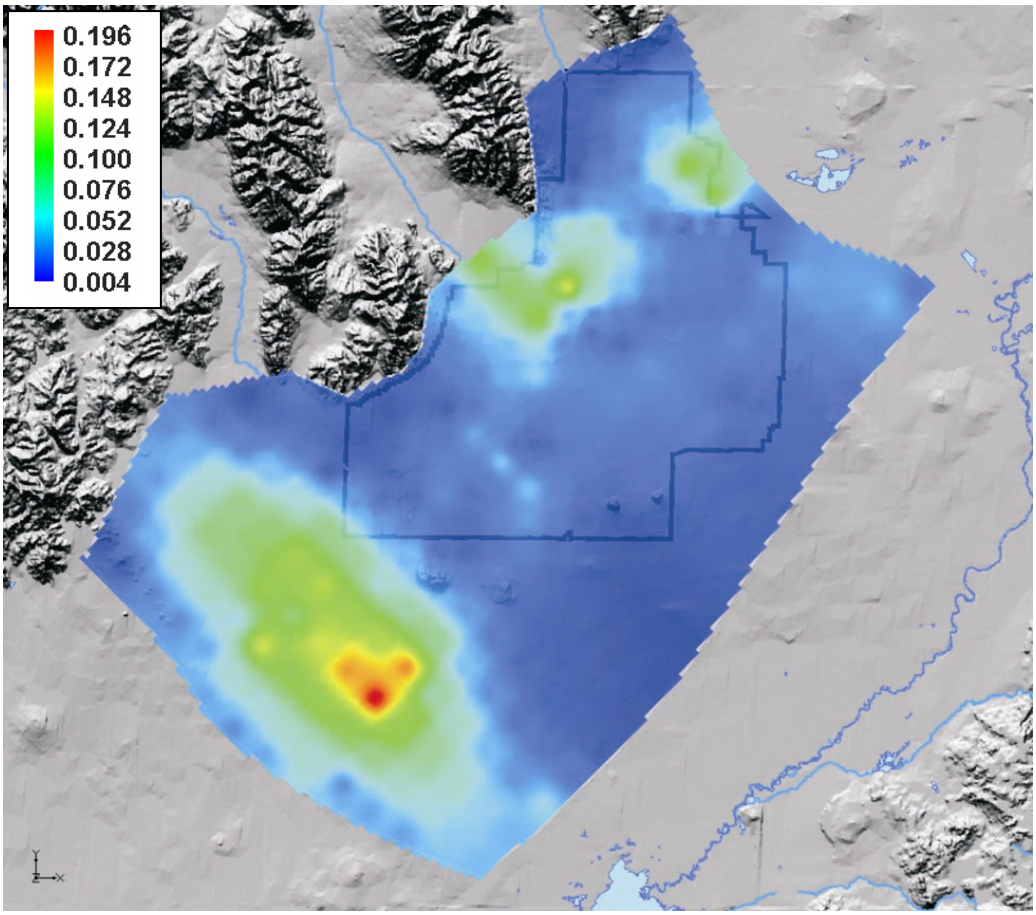

Figure 3-26. Spatial distribution of the composite sensitivity of hydraulic conductivity to the simulated heads.

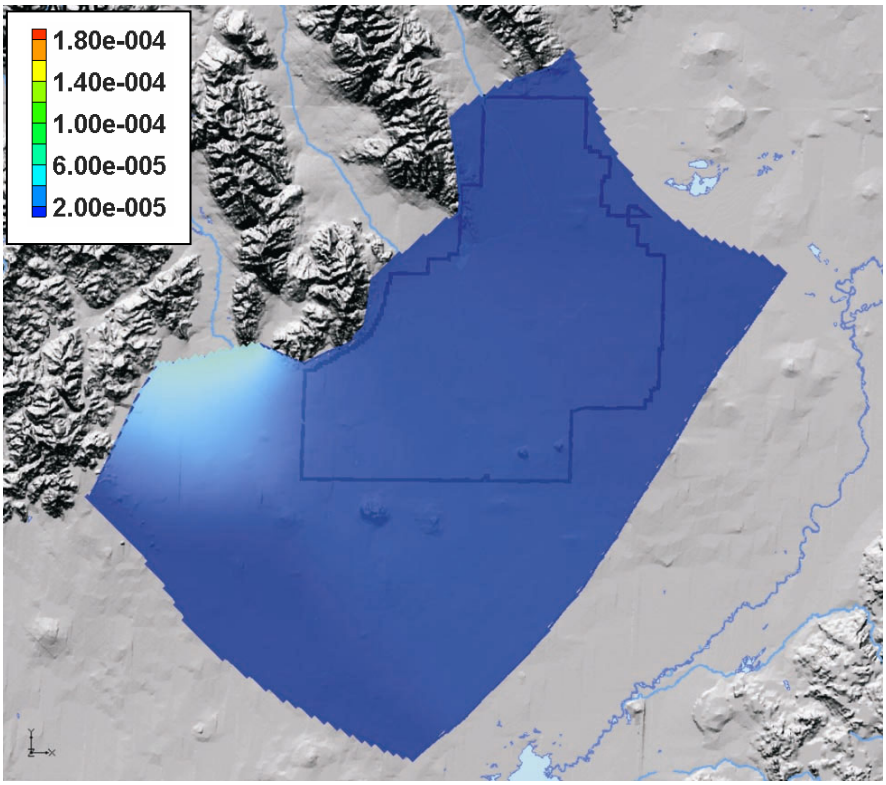

Figure 3-27. Sensitivity of the simulated heads to the underflow rate of the Big Lost River drainage basin.

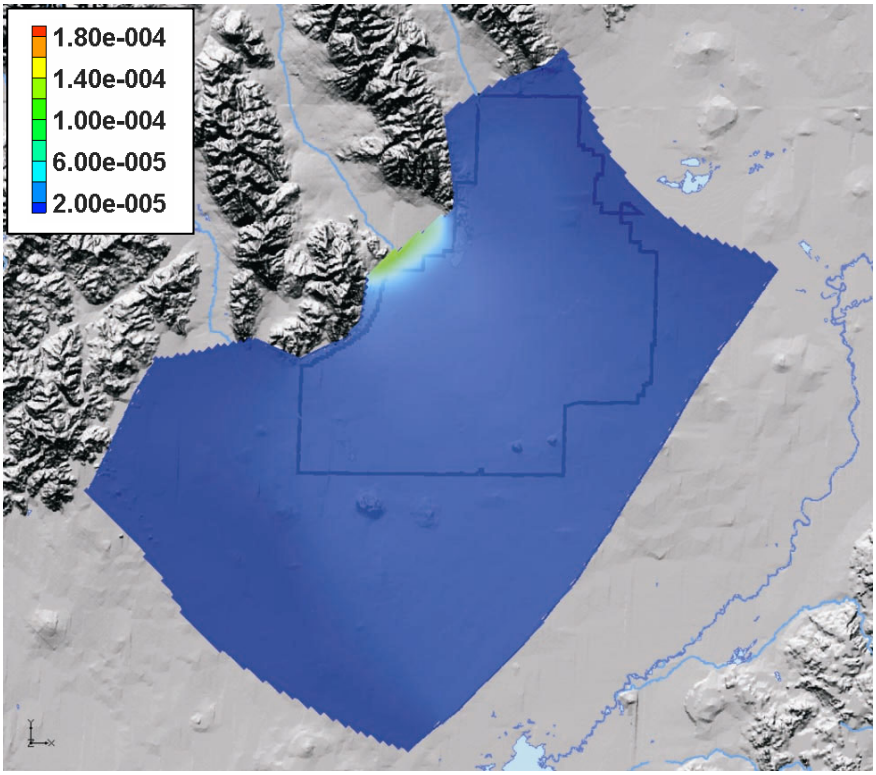

Figure 3-28. Sensitivity of the simulated heads to the underflow rate of the Little Lost River drainage basin.